Bismuth-modified vanadyl pyrophosphate catalysts

Y.H. Taufiq-Yap[a,*], K.P. Tan[a], K.C. Waugh[b], M.Z. Hussein[a], I. Ramli[a], and M.B. Abdul Rahman[a]

[a]*Department of Chemistry, Universiti Putra Malaysia, 43400 UPM Serdang, Selangor, Malaysia*
[b]*Department of Chemistry, University of Manchester Institute of Science and Technology, PO Box 88, Manchester, M60 1QD, United Kingdom*

Received 14 November 2002; accepted 1 May 2003

A 1% bismuth-doped VPO catalyst was prepared by refluxing $Bi(NO_3)_3$ and $VOPO_4 \cdot 2H_2O$ in isobutanol. The incorporation of Bi into the VPO lattice lowered the overall V oxidation state from 4.24 to 4.08. It also lowered both the peak maximum temperature for the desorption of oxygen from the lattice from 1001 K (undoped) to 964 K with a shoulder at 912 K and the peak maxima for H_2 temperature-programed reduction from 863, 1011 and 1143 K (undoped) to 798, 906 and 1151 K. The total oxygen desorbed from the Bi-doped catalyst was only one-fourth that of the undoped catalyst, while the amount of oxygen removed by TPR was roughly the same for both catalysts. These results suggest that in anaerobic oxidation, the Bi-doped catalyst will have roughly the same activity as in undoped catalyst in C_4 hydrocarbon oxidation but will have a higher selectivity to products such as olefins and maleic anhydride.

KEY WORDS: vanadyl pyrophosphate; promoter; bismuth; butane oxidation; maleic anhydride.

1. Introduction

Vanadium phosphorus oxide (VPO) is the commercial catalyst for the selective oxidation of butane to maleic anhydride. It is, so far, the only successful industrial process utilizing alkanes [1,2]. It is considered that the main active phase in catalysts stabilized under reaction conditions is $(VO)_2P_2O_7$, which is formed topotactically from the precursor $VOHPO_4 \cdot 0.5H_2O$ that can be prepared by a number of methods [3]. One of the methods of preparation is by the reduction of $VOPO_4 \cdot 2H_2O$, the catalyst resulting from which is found to be particular effective for *n*-butane oxidation. Catalytic performance may be improved by adding specific doping agents to the VPO composition. The nature, the location and the role of these dopants have been previously reviewed [4]. Several different metals have been used as the modifier, and data has been published on their influence on the yield and selectivity of formation of maleic anhydride, and on the reaction rate of these catalysts [5,6]. A somewhat recent publication was concerned not only with general aspects of the reaction of modified VPMO catalysts (where M stands for metal promoter) but also with the effect of modifiers on the structure and morphology of the catalysts in optimizing selective butane oxidation to maleic anhydride [7].

In general, promoters only constitute a small part of the overall composition of VPO catalysts [8]. Bismuth (Bi) has been used as a promoter by some researchers [9–11], showing an increase in selectivity to MA upon the addition of Bi. For the most advantageous performance properties, it is preferred that the total atomic ratio of Bi to the proportion of vanadium should be in the range of 0.001 : 1 to 0.2 : 1, preferably 0.005 : 1 to 0.07 : 1 [10]. Furthermore, X-ray diffraction (XRD) studies have shown that the Bi-doped materials are predominantly $(VO)_2P_2O_7$ with a minor amount of $BiPO_4$ [12].

A bismuth additive was introduced into VPO catalyst as bismuth chloride, but a yield of only 37% was found with this catalyst [8]. Haber *et al.* [13] have studied the effect of bismuth additive introduced into the VPO precursor, which was prepared in a classical organic medium. The Bi-doped catalyst gave an *n*-butane conversion of 76% and selectivity of 68% after the catalytic tests. A VPBiO catalyst is also used in *n*-pentane partial oxidation [14].

In this paper, the physical and chemical modifications induced in a vanadyl pyrophosphate catalyst will be examined.

2. Experimental

2.1. Preparation of doped vanadyl pyrophsophate catalysts

The undoped $VOHPO_4 \cdot 0.5H_2O$ precursor was prepared via $VOPO_4 \cdot 2H_2O$ (denoted as VPD method). V_2O_5 (12.0 g from Fisher Scientific) and *ortho*-phosphoric acid H_3PO_4 (115 g, 85% from Fisher) were refluxed in water (24-mL H_2O/g solid) for 24 h. The resulting $VOPO_4 \cdot 2H_2O$ was recovered by filtration and washed with water and finally identified by XRD. This solid (4 g) was then refluxed with isobutanol (80 mL from BDH) for 21 h, and the resulting solid was recovered by filtration and dried in air (383 K, 16 h).

* To whom correspondence should be addressed.

1011-372X/03/0700–0087/0

For the preparation of the Bi-doped precursor, the required mass of the bismuth nitrate salt was previously dissolved in isobutanol, prior to refluxing it with $VOPO_4 \cdot 2H_2O$ in isobutanol. The doped precursor was denoted PVPDBi1.

The resulting precursors were then calcined in a reaction flow of *n*-butane/air mixture for 75 h at 673 K. The activated doped catalyst was denoted VPDBi1.

2.2. Catalysts characterization

The total surface area and porosity of the catalysts were measured by the BET (Brunauer–Emmer–Teller) method using nitrogen adsorption at 77 K. This was done by the Micromeritics ASAP 2000 nitrogen adsorption/desorption analyzer.

The bulk chemical composition was determined by using a sequential scanning inductively coupled plasma-atomic emission spectrometer (ICP-AES) Perkin Elmer Emission Spectrometer model Plasma 1000. Each sample was digested by concentrated nitric acid (8 M) with slow heating. The resulting solution was diluted with distilled water to 250 mL.

The average oxidation state of vanadium in the catalysts were determined by redox titration following the method of Niwa and Murakami [15]. About 0.1 g of each catalyst was dissolved in 100 mL of 2 M H_2SO_4 at 353 K. The vanadium (IV or III) content was determined by titration with a solution of $KMnO_4$ (0.01 N). The vanadium (V) content was determined by titration with a solution of a Mohr salt ($FeSO_4 \cdot (NH_4)_2SO_4 \cdot 6H_2O$, 0.01 N) using diphenylamine as an indicator.

The XRD analyses were carried out using a Shimadzu diffractometer model XRD 6000 employing Cu Kα radiation to generate diffraction patterns from powder crystalline samples at ambient temperature.

SEM was done using a Jeol JSM-6400 electron microscope. The samples were coated with gold using a Sputter Coater. The photographs were captured using a Mamiya camera with Kodak Verichrome Pan 100 black and white negative film at various magnifications.

TPD (temperature-programmed desorption) and TPR (temperature-programmed reduction) analyses were done by using a ThermoFinnigan TPDRO 1110 apparatus utilizing a thermal conductivity detector (TCD).

3. Results and discussion

3.1. BET surface area measurement, chemical analysis and redox titration

The Bi-doped catalyst, VPDBi1, had a higher surface area, 25.0 $m^2 g^{-1}$, than that of VPD (20.3 $m^2 g^{-1}$). Doping with Bi has somehow altered the development of the basal (100) $(VO)_2P_2O_7$ face, which is the interesting feature of the high BET area of the catalyst. The addition of Bi cation into the VPD matrix has encouraged the formation of crystal phases with higher surface area. Chemical analysis using ICP indicated that the P/V ratio for VPD and VPDBi1 are 1.09 and 1.12 respectively, and confirmed the presence of Bi with a Bi/V atomic ratio of 0.0096.

The average oxidation number and percentage of V^V and V^{IV} oxidation state is shown in table 1. Bi was found to decrease the average oxidation number from 4.24 to 4.08, i.e., a reduction of V^V oxidation state in VPD from 24 to 8%.

3.2. X-ray diffraction (XRD)

XRD patterns of both precursors (figure 1) are identical to $VOHPO_4 \cdot 0.5H_2O$ with peaks at $2\theta = 15.75$, 19.83, 24.42, 27.28 and 30.63°. The XRD patterns for VPD and VPDBi1 catalysts are shown in figure 2 and these materials have similar patterns to a well-crystallized $(VO)_2P_2O_7$, with main peaks appearing at $2\theta = 22.9$, 28.4 and 29.3°, which correspond to (020), (204) and (221) planes respectively [16]. The addition of Bi leads to the reflection at $2\theta = 22.9°$ indexed to the (020) plane being more intense compared to the undoped catalyst. Our lack of observation of a separate $BiPO_4$ phase at a Bi : V ratio of 0.0096 would suggest that no $BiPO_4$ phase was formed and that all of the Bi was incorporated into the $(VO)_2P_2O_7$ lattice. This is implied in the finding by Ayub *et al.* [12] of a predominantly $(VO)_2P_2O_7$ crystal with a minor $BiPO_4$ phase for higher loadings, suggesting that the majority of the Bi was incorporated into the $(VO)_2P_2O_7$ lattice. Obviously, since the Bi^{3+} is much larger than V^{4+} (Bi^{3+} radius 103 pm; V^{4+} radius 58 pm), replacing a V^{4+} with Bi^{3+} will cause considerable strain in the lattice. This strained lattice would be suspected to release oxygen at a lower temperature (see below) and so increase both activity and selectivity.

Table 2 shows the line width of the (020) and (204) plane reflections. The parameter used to determine the crystal size is the half width of the (020) peak. The line width increases with the decreasing size of the crystallites [17]. The decrease in the FWHMs of the (020) reflection indicates that the thickness of the particles in the (100) direction decreases. The half width of the (204)

Table 1
Average oxidation numbers and percentages of V^V and V^{IV} oxidation states present in VPD and VPDBi1

Catalyst	V^V (%)	V^I (%)	Average oxidation number
VPD	24	76	4.24
VPDBi1	8	92	4.08

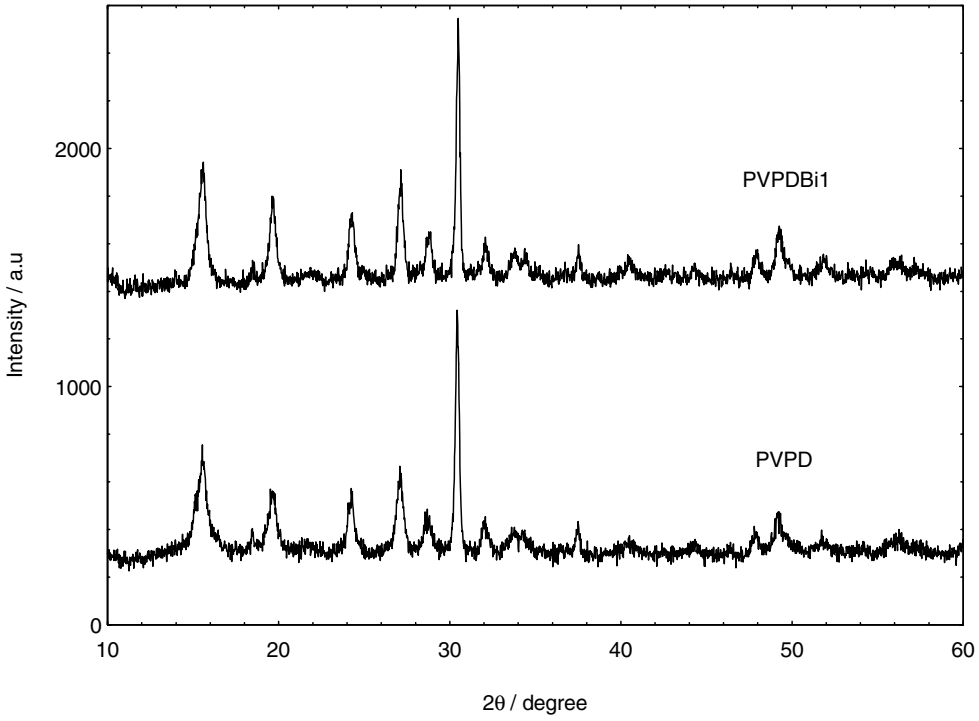

Figure 1. XRD patterns of PVPD and PVPDBi1.

peak changes slightly, reflecting a constant crystalline order of the *bc* plane, as well.

The particle thickness is given by the Debye–Scherrer equation:

$$t = \frac{0.9\lambda}{\beta_{hkl}\cos\theta_{hkl}}$$

where t is the particle thickness for the (hkl) phase, λ is the X-ray wavelength of radiation for Cu Kα, β_{hkl} is the full width at half maximum (FWHM) at the (hkl) peak and θ_{hkl} is the diffraction angle for the (hkl) phase [18]. The particle thickness for VPD at (020) and (204) were, as calculated from the above formula, 69.09 and 173.62 Å respectively (table 2). However, the particle

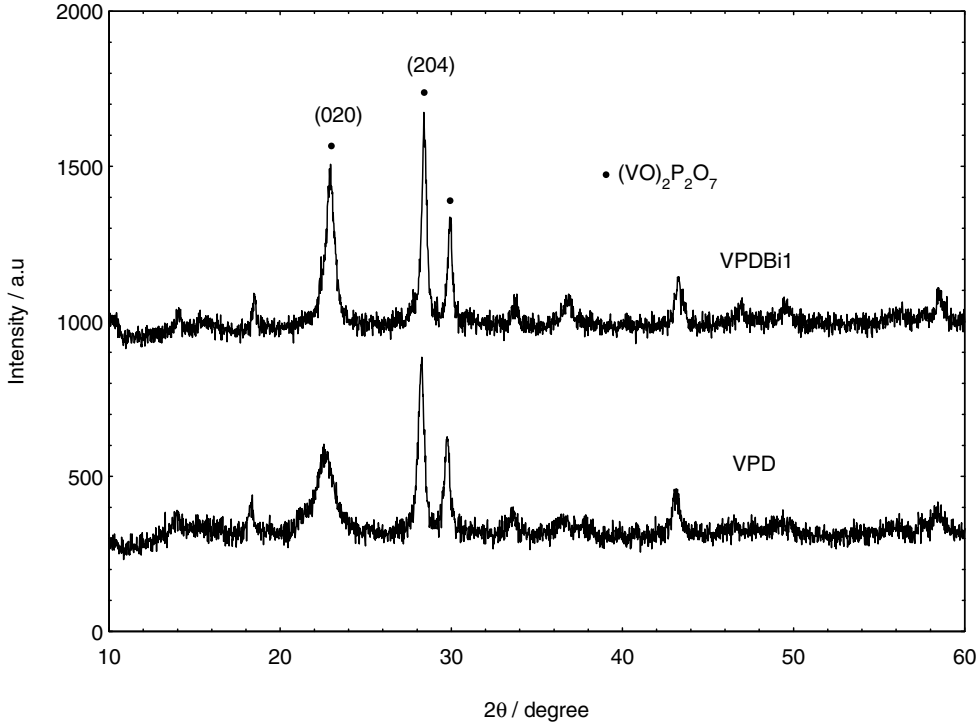

Figure 2. XRD patterns of VPD and VPDBi1.

Table 2
XRD data of undoped and doped VPD catalysts

Catalyst	Line width[a] (020)/Å	Line width[b] (204)/Å	Thickness[c] (020)/Å	Thickness[c] (204)/Å
VPD	1.1600	0.4616	69.09	173.62
VPDBi1	0.5873	0.3541	136.46	226.32

[a]FWHM of (020) reflection.
[b]FWHM of (204) reflection.
[c]Plate thickness by means of Scherrer's formula: $T(\text{Å}) = (0.89 \times \lambda)/(\text{FWHM} \times \cos\theta)$.

thickness of (020) and (204) for the Bi-doped VPD catalyst were both increased to 136.46 and 226.32 Å respectively.

3.3. Scanning electron microscopy (SEM)

The morphology of the undoped and Bi-doped VPD catalysts is shown in figure 3. The principle structure of the catalysts is the same, consisting of platelike crystals, which are arranged into the characteristic rosette-shaped clusters [19]. The undoped VPD catalyst shows a rosette-type structure with a crystallite of uniform size.

However, Bi-doped catalyst showed more layered platelike crystals, which form at the surface of clusters. This could explain why the Bi-doped catalyst had a higher surface area than VPD. The layered structure increased the exposure of the basal (100) $(VO)_2P_2O_7$ face. The rosette-type agglomerates are made up of $(VO)_2P_2O_7$ agglomerates of platelets that are preferentially exposing (100) crystal planes [20].

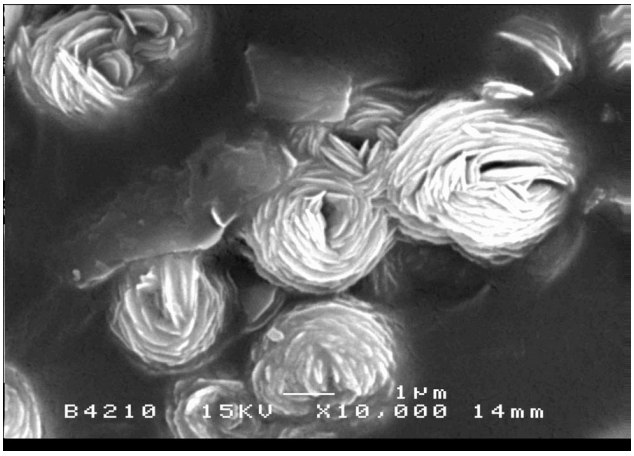

(a)

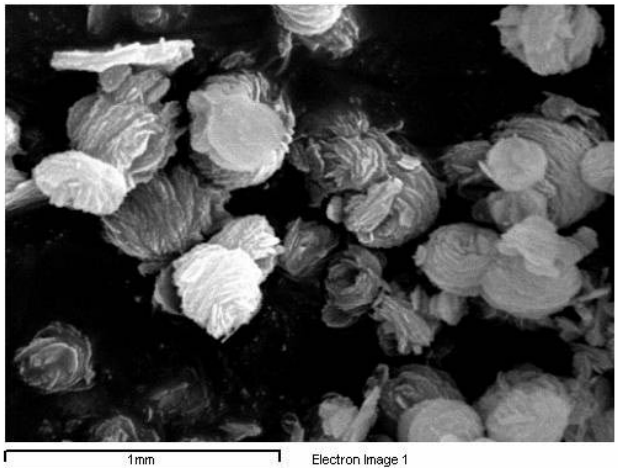

(b)

Figure 3. SEM micrographs of (a) VPD and (b) VPDBi1 catalysts.

3.4. O_2 temperature-programed desorption (TPD)

The oxygen desorption spectra for VPD and VPDBi1 catalysts shown in figure 4 were carried out by pretreating the catalysts by heating them to 673 K in an oxygen flow (1 bar, 25 cm^3 min^{-1}), holding it under that stream at 673 K for 1 h, before cooling it to ambient. Then the flow was switched to helium and the temperature was raised to 1223 K (20 K min^{-1}) following the conductivity of the oxygen by a thermal conductor detector. The onset of O_2 evolution for VPDBi1 occurs at $\sim$ 810 K with a peak maximum observed at 964 K and a shoulder at 912 K. However, VPD gave only one higher temperature (37 K higher) peak at 1001 K with an onset oxygen peak at $\sim$ 840 K. These are assigned to the lattice oxygen, which also has been observed earlier in organic method preparation of the VPO catalyst [21]. The addition of Bi significantly reduced the lattice oxygen desorption temperature by $\sim$ 89 K.

The total amount of oxygen desorbed from VPDBi1 is 9.45×10^{19} atom g^{-1} corresponding to a coverage of 3.78×10^{14} atom cm^2, which is equivalent to $\sim$ 0.54% of the lattice oxygen. This amount is only one quarter of the undoped catalyst (table 3).

The desorption activation energy for the peak at 1001 K for VPD corresponds to 276.4 kJ mol^{-1} (table 3), whereas peaks for VPDBi1 at 912 K and 963 K correspond to 251.8 and 266.2 kJ mol^{-1} respectively. The desorption activation energies were obtained by solution of the Redhead equation [22],

$$\frac{E_d}{\mathrm{RT}_m{}^2} = \left(\frac{A}{\beta}\right)\exp\left(\frac{-E_d}{\mathrm{RT}_m}\right)$$

where E_d is the desorption activation energy (kJ mol^{-1}), A is the desorption A-factor (10^{13}/s, assumed), R is the gas constant (J/K/mol), β is the heating rate (K/s) and T_m (K) is the temperature of the peak maximum.

3.5. Temperature-programed reduction (TPR)

Figure 5 shows the TPR profile in a H_2/Ar stream (5% H_2 in Argon, 1 bar, 25 cm^3 min^{-1}), using a fresh

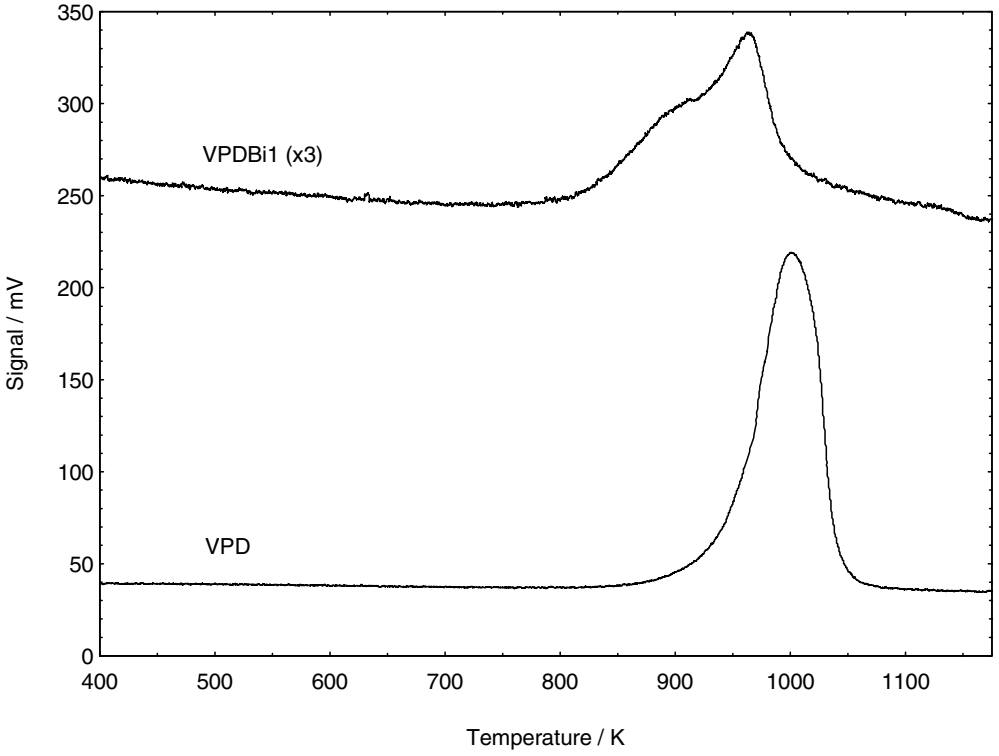

Figure 4. TPD of O_2 for VPD and VPDBi1 catalysts.

sample of catalyst and raising the temperature from ambient to 1223 K at 20 K min^{-1} in that stream.

Three distinct peaks maxima of VPD were observed in the rate of hydrogen consumption at 863, 1011, and 1143 K (table 4), whereas Bi-doped catalyst also gave three peaks maxima. However, the first two peaks maxima were significantly shifted to a lower temperature, i.e., 798 and 906 K. The reduction temperature of oxygen removed from the lattice by reaction of H_2 is consistent with the observation of oxygen evolution from the lattice thermally.

The total amount of H_2 consumed is 2.53×10^{21} atom g^{-1} for VPD catalyst and 2.78×10^{21} atom g^{-1} for VPDBi1 catalyst, which correspond to $\sim 14.4\%$ and $\sim 15.8\%$ oxygen atoms removed from the lattice respectively. The values of the activation energies are obtained from a modified version of the Redhead equation,

$$\frac{E_r}{\mathrm{RT}_m{}^2} = \left(\frac{A_r}{\beta}\right)[\mathrm{H_2}]_\mathrm{m} \exp\left(\frac{-E_r}{\mathrm{RT}_m}\right)$$

where T_m is the peak maximum temperature (K) in the rate of consumption of H_2, E_r is the reduction activation energy (kJ mol^{-1}), A_r is the reduction pre-exponential term (cm^3 mol^{-1} s^{-1}) that is given the value of a standard collision number of 10^{13} cm^3 $mol^{-1}s^{-1}$ and $[H_2]_\mathrm{m}$ is the gas-phase concentration of hydrogen (mol/cm^3) at the maximum peak [23]. The reduction activation energies for VPD, as such, are calculated to be (i) 144.3 kJ mol^{-1} at 863 K, (ii) 169.1 kJ mol^{-1} at 1011 K and (iii) 191.1 kJ mol^{-1} at 1143 K. Also, the

Table 3
Amount of oxygen desorbed and desorption activation energies obtained by temperature-programmed desorption from VPD and VPDBi1 catalysts

Peaks	T_max(K)	Desorption activation energy, E_d (kJ mol^{-1})	Total amount of oxygen atoms desorbed (mol g^{-1})	Total amount of oxygen atoms desorbed (atom g^{-1})	Coverage (atom cm^2)
VPD					
1	1001	276.4	5.12×10^{-4}	3.08×10^{20}	1.52×10^{15}
VPDBi1					
1	912	251.8	1.42×10^{-4}	8.55×10^{19}	3.42×10^{14}
2	964	266.2	1.50×10^{-5}	9.03×10^{18}	3.61×10^{13}
Total oxygen atoms desorbed			1.57×10^{-4}	9.45×10^{19}	3.78×10^{14}

Note: Surface area: VPD = 20.26 m^2 g^{-1}; VPDBi1 = 25.03 m^2 g^{-1}; weight:VPD = 0.0861 g; VPDBi1 = 0.0842 g.

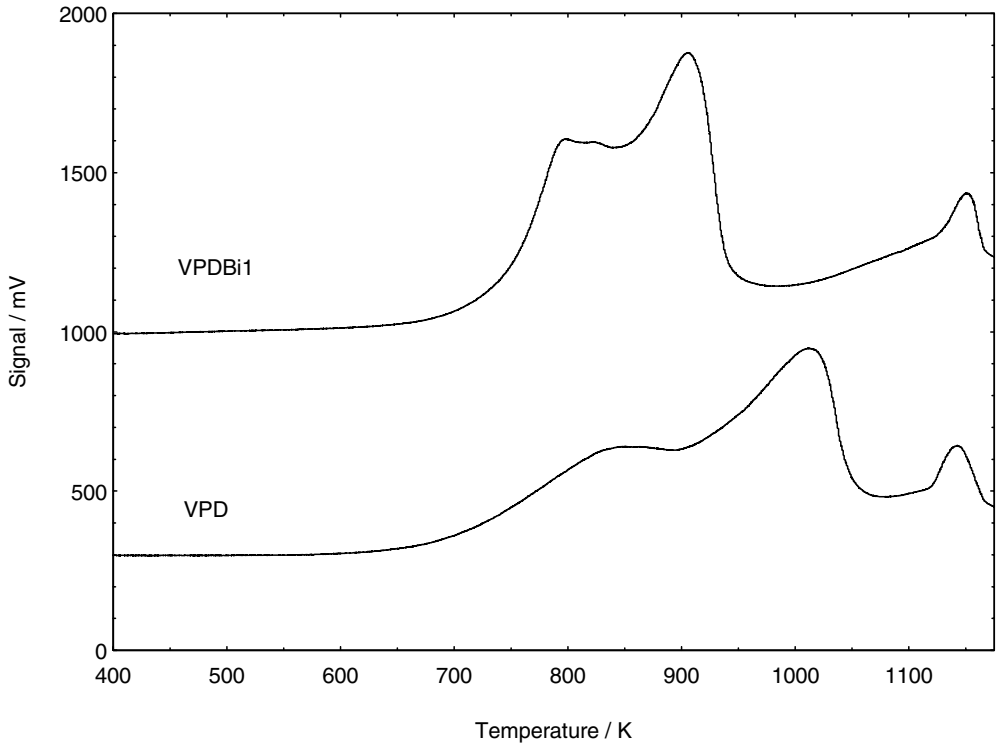

Figure 5. TPR for VPD and VPDBi1 catalysts.

Table 4
Total number of oxygen atoms removed from the VPD and VPDBi1 catalysts by reduction in H_2/Ar

Peaks	T_{max}(K)	Reduction activation energy, E_r (kJ mol^{-1})	Oxygen atoms removed from the catalyst (mol g^{-1})	Oxygen atoms removed from the catalyst (atom g^{-1})	Coverage (atom cm^2)
VPD					
1	863	144.3	1.35×10^{-3}	8.13×10^{20}	4.01×10^{15}
2	1011	169.1	2.10×10^{-3}	1.26×10^{21}	6.22×10^{15}
3	1143	191.1	7.58×10^{-4}	4.56×10^{20}	2.25×10^{15}
Total oxygen atoms removed			4.21×10^{-3}	2.53×10^{21}	1.25×10^{16}
VPDBi1					
1	798	133.5	1.44×10^{-3}	8.67×10^{20}	3.46×10^{15}
2	906	151.5	1.85×10^{-3}	1.11×10^{21}	4.44×10^{15}
3	1151	192.5	1.33×10^{-3}	8.01×10^{20}	3.20×10^{15}
Total oxygen atoms removed			4.62×10^{-3}	2.78×10^{21}	1.11×10^{16}

Note: Surface area: VPD = 20.26 m^2 g^{-1}; VPDBi1 = 25.03 m^2 g^{-1}; weight: VPD = 0.0379 g; VPDBi1 = 0.0375 g.

activation energy values for VPDBi1 are (i) 133.5 kJ/mol at 798 K, (ii) 151.5 kJ/mol at 906 K and (iii) 192.5 kJ/mol at 1151 K.

4. Conclusions

1. The physical effect of the incorporation of Bi (1%) into a VPO lattice is an increase in the total surface area of the catalysts from 20.3 m^2 g^{-1} (undoped) to 25 m^2 g^{-1}. This increase in area is brought about by an increase in the rosette-type platelets subtending the (100) face.

2. The chemical effects of the incorporation of Bi into the VPO lattice are (i) a reduction in the overall oxidation state of the vanadium from 4.24 to 4.08 and (ii) a reduction in its activation energy for the desorption of oxygen from the lattice and a lowering in the activation energy for the reduction of the lattice with H_2. We have previously suggested that there is a correlation between the H_2 reduction kinetics and its selectivity of the catalyst in butane oxidation [24].

Acknowledgment

The authors are indebted to Dr. L. Lucarelli (ThermoFinnigan, Italy) for the TPD and TPR experiments. Financial assistance from the Malaysian Minis-

try of Science, Technology and Environment is gratefully acknowledged.

References

[1] D.X. Wang, M.C. Kung and H.H. Kung, Catal. Lett. 65 (2000) 9.
[2] G. Centi, Catal. Today 16 (1993) 1–153 (the entire volume).
[3] I.J. Ellison, G.J. Hutchings, M.T. Sananes and J.C. Volta, J. Chem. Soc., Chem. Commun. 1093 (1994).
[4] G.J. Hutchings, Appl. Catal. 72 (1991) 1.
[5] M. Brutovský, D. Kladeková and A. Kosturiak, Chem. Listy 89 (1995) 682.
[6] V.A. Zazhigalov, Kataliz, Katalizatory 25 (1987) 12.
[7] D. Kladeková, A. Hanudel, M. Brutovský and J. Novak, Collect. Czech. Chem. Commun. 60 (1995) 457.
[8] B.K. Hodnett, Catal. Rev. Sci. Eng. 27(3) (1985) 373.
[9] A. Bortinger, US Patent 5,885,919 (1999) assigned to Scientific Design Company, Inc.
[10] C.J. Edwards, US Patent 4,515,904 (1995) assigned to Standard Oil Company (Indiana).
[11] S.H. Sookraj and D. Engelbrecht, Catal. Today 49 (1999) 161.
[12] I. Ayub, D.S. Su, M. Willinger, A. Kharlamov, L. Ushkalov, V.A. Zazhigalov, N. Kirillova and R. Schlogl, Phys. Chem. Chem. Phys. 5 (2003) 970.
[13] J. Haber, V.A. Zazhigalov, J. Stoch, L.V. Bogutskaya and I.V. Batcherikova, Catal. Today 33 (1997) 39.
[14] V.A. Zazhigalov, J. Haber, J. Stoch and E.V. Cheburakova, Catal. Commun. 2 (2001) 375.
[15] M. Niwa and Y. Murakami, J. Catal. 76 (1982) 9.
[16] Y.H. Taufiq-Yap, K.C. Waugh and M.Z. Hussein, Oriental J. Chem. 14(1) (1008) 1.
[17] L.M. Cornaglia, C.R. Carrara, J.O. Petunchi and E.A. Lombardo, Appl. Catal., A: Gen. 183 (1999) 177.
[18] P.H. Klug and E. Alexander, *X-ray Diffraction Procedures for Polycrystalline and Amorphous Materials*, 2nd ed. (1974).
[19] Y.H. Taufiq-Yap, M.H. Looi, K.C. Waugh, M.Z. Hussein, Z. Zainal and R. Samsuddin, Catal. Lett. 74(1-2) (2001) 99.
[20] C.J. Kiely, S. Sajip, I.J. Ellison, M.T. Sananes, G.J. Hutchings and J.C. Volta, Catal. Lett. 33 (1995) 357.
[21] B.H. Sakakini, Y.H. Taufiq-Yap and K.C. Waugh, J. Catal. 189 (2000) 253.
[22] P.A. Redhead, Vaccum 12 (1962) 203.
[23] J.W. Niemantsverdriet, *Spectroscopy in Catalysis* (VCH Verlagsgesellschaft, Weinheim, 1993).
[24] Y.H. Taufiq-Yap, M.H. Looi, K.C. Waugh, M.Z. Hussein, Z. Zainal and R. Samsuddin, Catal. Lett. 74 (2001) 99.